Pereira Rui (Orcid ID: 0000-0002-5105-5082)

Gentili Chiara (Orcid ID: 0000-0001-6745-3782)

Beta tricalcium phosphate ceramic triggers fast and robust bone formation by human mesenchymal stem cells

R.C. Pereira[1†], R. Benelli[2], B. Canciani[1], M. Scaranari[1], G. Daculsi[3], R. Cancedda[1], C. Gentili[1*,4]

[1]Laboratory of Regenerative Medicine, Department of Experimental Medicine (DIMES)-University of Genoa, Largo Rosanna Benzi 10, Genoa 16132 Italy
[2]Laboratory of Immunology, IRCCS AOU San Martino – IST Largo Rosanna Benzi 10, 16132 Genoa, Italy
[3]INSERM LIOAD U791, Nantes University, Dental Faculty, place Alexis Ricordeau, 44042 Nantes France
[4]Centre of Excellence for Biomedical Research (CEBR), University of Genova, Viale Benedetto XV 9, 16132 Genova, Italy.

Keywords: Calcium phosphate, Osteogenesis, Vascularization, Regenerative Medicine

Running title: **Beta tricalcium phosphate (triggers) robust bone formation**

†Present address: R. C. Pereira, Laboratory of Neurobiology of miRNAs laboratory, Fondazione Istituto Italiano di Tecnologia, Via Morego, Genova, Italy

This article has been accepted for publication and undergone full peer review but has not been through the copyediting, typesetting, pagination and proofreading process which may lead to differences between this version and the Version of Record. Please cite this article as doi: 10.1002/term.2848

* Corresponding Author: **Chiara Gentili**

Department of Experimental Medicine (DIMES), University of Genoa, Italy

Largo Rosanna Benzi 10, 16132 Genova, Italy

Telephone number: +39-010-5558241

Fax number: +39-010-5558257

Email address: chiara.gentili@unige.it

Abstract

Due to their osteoconductive and inductive properties, a variety of calcium phosphate (CaP) scaffolds are commonly used in orthopaedics as graft material to heal bone defects. In this study, we have used two CaP scaffolds with different hydroxyapatite (HA) and β-tricalcium phosphate (β-TCP) ratios (MBCP®; 60/40 and MBCP+®; 20/80), to investigate their intrinsic capacity to favour human bone marrow stem cells (hBMSC) osteogenic differentiation capacity. We report that MBCP+® showed in *in vitro* culture model a higher rate of calcium ion release in comparison with MBCP®. In two defined co-culture systems, the hBMSC seeded onto MBCP+® presented an increased amount of VEGF secretion, resulting in an enhanced endothelial cell proliferation and capillary formation compared to hBMSC seeded onto MBCP®. When both ceramics combined with hBMSC were implanted in a nude mouse model, we observed a faster osteogenic differentiation and enhancement mature bone deposition sustained by the presence of a vast host vasculature within the MBCP+® ceramics. Bone formation was observed in samples highly positive to the activation of Calcium sensing receptor protein (CaSr) on the surface of seeded hBMSC that also shown higher BMP-2 protein expression. With these data we provide valuable insights in the possible mechanisms of ossification and angiogenesis by hBMSC that we believe to be primed by calcium ions released from CaP scaffolds. Evidences could lead to an optimization of ceramic scaffolds to prime bone repair.

Introduction

Canonical tissue engineering approaches involve seeding of stem cells onto properly designed biomaterials to induce cellular differentiation through pre-defined pathways with tissue regeneration as the final target (Quarto, 2003; Oreffo & Triffitt, 1999). For bone repair, synthetic calcium phosphate (CaP) ceramic scaffolds have been used as graft substitutes because the chemical composition resembles the bone mineral phase (Espitalier et al., 2009; Komlev et al., 2010; LeGeros, 2008; Mastrogiacomo et al., 2006). Maximization of osteoconductive and osteoinductive properties of CaP scaffolds is one of the main objectives to better apply ceramics in bone tissue engineering (A M C Barradas, Yuan, van Blitterswijk, & Habibovic, 2011; G Daculsi, Laboux, Malard, & Weiss, 2003; Komlev et al., 2010). Parameters like chemical composition, micro and macro porosity are involved in osteoinductive properties, and macroporosity in osteogeneic capacity of MSC differentiation (niche concept) are optimized to achieve better clinical outcomes (A M C Barradas et al., 2012; Guy Daculsi, 2015; Guy Daculsi & Layrolle, 2004). Over the last few years, the role of CaP scaffolds has been changing from a structural passive function to one in which the intrinsic properties act as fundamental key in the whole orchestra of tissue regeneration (Daculsi et al., 2013; Liu et al., 2004; Le Nihouannen et al., 2005; Place et al., 2009; Tampieri et al., 2011). When ceramics are used as vehicles to deliver human bone mesenchymal stromal cells (hBMSC) to trigger de novo bone formation, seeded cells and the host recipient microenvironment are crucial for the implant success. The complex process needed to formation of a new and organized host vasculature during bone repair is influenced by several events including interaction of different types of cells and the release of soluble factors, cytokines and matrix macromolecules (S Ghanaati et al., 2011; Novosel, Kleinhans, & Kluger, 2011). Among these, vascular endothelial growth factor (VEGF) plays an important role in the cascade of events that guides the bone formation and maturation, i.e. by direct

intramembranous ossification or by endochondral ossification (Ferrara, Gerber, & LeCouter, 2003; Kanczler & Oreffo, 2008; Novosel et al., 2011). Likewise, the dissolution of ceramics main elements, e.g. calcium (Ca^{2+}) and phosphate (PO^{4}_{3-}), has an important role on osteogenesis in which diverse mechanisms are linked to cell sensibility to external Ca^{2+} variations. Calcium can enter the cell membranes through G-protein coupled receptors (GPCRs) (A M Hofer & Lefkimmiatis, 2007; Matsubara et al., 2008; Yao et al., 2014). Realize an *in vivo* regulation of BMP-2 expression and secretion in hBMSC seeded onto CaP ceramics, via modification of the extracellular Ca^{2+} concentration, could lead to clarify mechanisms that would re-direct strategies in bone tissue engineering.

Herein we have; i) investigated how hBMSC seeded onto two different types of CaP ceramic scaffolds regulate proliferation and function of HUVEC cells *in vitro*; ii) studied how ions released from CaP scaffolds could prime the ossification process of hBMSCs; iii) analysed how CaP scaffolds could influence *in vivo* ossicle formation and maturation and at the same time the engraftment of host endothelial cells in the implanted scaffolds.

Materials and Methods

Calcium phosphate characterization

Calcium phosphate ceramic scaffolds were provided by Biomatlante SA (Vigneux-de-Bretagne, France) under EU GAMBA-Project from FP7 framework (NMP3-Sl-2010-245993). The macro and microstructure of the different ceramics was evaluated using Scanning electron microscope (SEM) (Leo 1450VP, Zeiss, Germany). Composition of ceramics (ratio of HA and β-TCP) was determined by X-ray diffraction (XRD) (Philips Analytical X ray BV diffractometer, Nederland) and Fourier transform infra-red spectroscopy (FTIR), (Nicolet Magnall, USA). Porosity was determined by Hg porosimetry (Micromeretics Autoport3), the SSA specific surface area using BET (ASAP 2010 Micromeritics), and mechanical testing by

TH HD plus Texture Analyseur made on calibrated samples (5mm in diameter and 8mm height). The micro/macro-porous sizes of the different ceramics were analysed in 3D using X-rays micro CT, using CT software for quantification.

Calcium release profile was determined by immersing 10 mg of 0.5-1 mm ceramic particles in 50 mL of simulated physiological saline solution (0.8% NaCl, 50 mM Hepes, pH 7.0) at 37 °C under constant agitation. Calcium content in the solutions at each time point for 240 minutes was monitored and quantified by a colorimetric assay kit (BioVision, CA, USA) according to the manufacture instructions.

Cell isolation and culture

1. Human Bone Marrow Stromal Cells

Human BMSC were derived from iliac crest marrow aspirates of healthy donors after informed consent. Human samples were obtained from EU-PurStem Consortium, after approval by the Clinical Research Ethical Committee at University College Hospital, Galway, Ireland. Briefly, cell-nucleated fraction of 20 mL bone marrow aspirate were suspended in Coon's modified Ham's F-12 medium (Biochrom) supplemented with 10% fetal calf serum (EuroClone), human recombinant fibroblast growth factor 2 (FGF-2) (1ng/mL) (Prepotech), 100 IU/mL penicillin and 100 mg/mL streptomycin, 2 mmol/L Lglutamine (EuroClone), and plated at a density of $1x10^6$ cells/cm^2 (Muraglia, Martin, Cancedda, & Quarto, 1998a). Medium was changed twice a week. When culture dishes were nearly confluent (passage 0), BMSC were detached with trypsin-EDTA (Gibco) and 0.5 x 10^6 cells were re-plated in 100 mm dishes (passage 1). At the next sub-confluence, cells were detached and $2.5x10^6$ BMSC seeded on the two different ceramics and implanted subcutaneously on the back of CD-1 nu/nu (Charles River – Calco, Lc, Italy) (Goshima, Goldberg, & Caplan, 1991). Three different BMSC primary cultures were tested with eight animals for each condition were implanted.

2. Human Umbilical Vein Endothelial Cells.

Human Umbilical Vein Endothelial Cells (HUVEC) were cultured in M199 medium (Gibco) supplemented with 10% FCS, Endothelial Growth Factor (EGF) 2 ng/ml (Prepotech), Heparin 10 μg/ml, and Hydrocortisone 10 μg/ml (Sigma). All cellular experiments were performed in a 5% CO_2 humid atmosphere at 37°C.

HUVEC proliferation and differentiation assays

hBMSCs were seeded on the ceramic scaffolds and cultured for 6 days. Afterwards, ceramics were extensively washed with PBS and placed in serum free medium (SF) for 2 days, demonstrated to be the optimal time to evaluate HUVEC response without cellular alterations. To co-culture BMSC with HUVEC, we used transwell system (Corning®). BMSCs were seeded onto ceramics at a cell density of $2.5x10^6$ cells/scaffolds and placed in the transwell lower chambers, whereas HUVEC ($5x10^3$ cells) were seeded in the transwell inserts (polycarbonate membrane with pore size 0.4 μm) previously coated with gelatin (10 mg/ml for 10 minutes at room temperature) (Figure 1A). After 2 days, cells were fixed with paraformaldehyde (PFA) 3.7% for 10 minutes, washed with PBS and stained with DAPI (10 mg/ml). Cells were counted in five ROIs for each condition.

HUVEC capillarity capacity was assessed using a similar non-direct co-culture system. Calcium phosphate ceramics seeded with hBMSC were placed at the bottom of 24 multi-wells. Matrigel (BD, UK) was added to the well plate (500 μl/well) in order to totally cover the calcium phosphate ceramics. After gelation at 37°C in a humidified atmosphere with 5% CO_2 for 10 minutes, 7×10^4 cells were layered on the top of Matrigel in 100 μl of DMEM (Fig. 2a). Capillary tube formation was measured after 6 and 24 hours, by counting the internodes of the capillary network formed. Values were normalized by the counted number of internodes formed in presence of CaP without hBMSCs. Huvec capillary tube formation in absence of

ceramic scaffolds was also made. Representative figures of the experiments are shown in Supplementary Figure 2.

VEGF quantification assay

hBMSCs were seeded onto the ceramics and kept in culture (Ham's F-12 complete medium) for 6 days. Thereafter, ceramics were washed extensively with PBS to remove FCS growth factors, and placed in 1 ml of serum free (SF) medium for 2 days. Conditioned media (CM) were collected and kept at -20°C until further analysis. VEGF present in the media was quantified by means of enzyme-linked immunosorbent assay (ELISA) (R&D Systems, UK) according to manufacturer's protocols.

Histology

Explanted samples were both decalcified and processed to obtain paraffin embedded, cryo-sections and non-decalcified samples. In brief, decalcified samples were PFA-fixed, decalcified with Osteodec (Bio-Optica, Milano, Italy) and embedded in paraffin or in OCT (Thermo Scientific, USA) using standard histological procedure. 4 µm serial sections were cut and sections were stained with haematoxylin and eosin (H&E). Cryo-sectioned samples were used for immune-fluorescence detection of BMP-2. For resin embedding, explanted and fixed calcium phosphate ceramics were infiltrated with the light-curing resin Technovit 7200VLC (Kulzer, Wehrheim, Germany) for 21 days under vacuum with resin replaced every 7 days. Samples were polymerized by the EXAKT 520 polymerization system (EXAKT Wehrheim, Bio-Optica, Italy) with curing performed with 450 nm light at temperature bellow 40°C. Samples were cut using EXAKT 310 CP cutting unit (EXAKT Wehrheim, Bio-Optica, Italy). Obtained sections were approximately of 150 µm in thickness. Samples were then grinded to 20–30 µm thickness using the EXAKT 400 CS micro grinding unit (EXAKT Wehrheim, Bio-

Optica, Italy). Sections were stained with Stevenel's/Van Gieson. For all processed ceramic samples, images were taken using Axiovert 200M microscope (Zeiss, Germany).

Vascular and bone histomorphometric assays

Calcium phosphate ceramics were fixed, decalcified and embedded in paraffin as described above. To visualize and quantify vascular structures in the calcium phosphate ceramics, 4 □m sections were cut and stained with Mallory's trichrome according to manufacturer's instructions (Bio-Optica). Five non-consecutive sections for each sample were observed in transmitted light. Image J64 software was used to quantify the number of vessels for each ROI through the followed steps: (i) vessel perimeter was manually defined; (ii) vessels were counted; (iii) number of vessels for ROI were determined. To quantify deposited bone, 4 □m sections were stained with H&E and analysed in transmitted light. Five non-consecutive sections for sample were analysed using Image J64 software to calculate bone matrix deposition area as follows: bone and scaffold areas were delimitated and the ratio between both areas converted to percentage of bone per ROI.

Immunohistochemistry

Immunoperoxidase was performed to detect human Calcium Sensing Receptor protein (CaSr) by the use of a rabbit anti-human CaSr antibody (1:250, Epitomics). Dako secondary anti-rabbit antibody and fluorochrome substrate solutions were used according to instructions. To identify human ALU-repeat-sequences, chromogenic in situ hybridization (CISH, Zytovision kit) was performed according to manufacturer's instructions. Immunolocalization of BMP-2 was made by the use of a polyclonal rabbit anti-human BMP-2 antibody (Santa Cruz Biotechnology) followed by DyLight 549 goat anti-rabbit antibody (Jackson Immunoresearch). Pre-immune

serum controls were run in parallel. All images were acquired using a phase-contrast Axiovert 200M microscope (Zeiss).

Ectopic bone formation by hBMSCs

Ectopic bone formation assay was made according to Muraglia et al. using $2x10^6$ of hBMSCs for each scaffold (Muraglia et al., 1998a). Groups of 8 animals were sacrificed at 7 days, 1 and 2 months. All animals were maintained as required by the Italian Ministry of Health in accordance with the standards of the Federation of European Laboratory Animal Science Associations (FELASA) (Animal Research Project N°336).

Statistical analysis

In vitro statistical analysis was performed using 1 way ANOVA (and Nonparametric) for Figure 1B; and two-tailed t-test for Figure 1d, 2, 3 and 4. Error bars indicate standard deviation (S.D.). In vivo statistical evaluation was done by using the data from explants of n=8 animals for each experimental condition. The data were analysed by two-tailed t-test. Error bars indicate standard deviation. For all in vitro and in vivo figures, a p-value 0.05 was considered to be statistically significant. All the statistical analysis of the acquired data was made using GraphPad software.

Results

MBCPs characterisation

XRD (single crystal X-ray diffraction) showed the high crystalline content of the granules with a ratio of 20% HA and 80% β-TCP for MBCP$^{+®}$ and 60/40 ratio for MBCP^{+}. The total porosity in both ceramics was of 70% with a distribution of 25% of micropores (less than 10 µm), 75% of mesopores and macropores (over 10 µm, mean size of macropores being 300-600 µm).

(Supplementary Figure 1A and B). The granules showed irregular shape with macro concavities. Supplementary table 1 shows the results of MicroCT and Hg porosity which does not reveal significant differences in the total porosity (75%). However, even without significative differences in the overall porosity values, zeta potential of MBCP® are almost three times more negative (-31.2 ± 0.4) than those observed in MBCP^{+}® (-13.6 ± 0.9), that could interfere with protein CaPs interactions.

In vitro calcium ions release profile

Calcium release was significantly higher in MBCP^{+}® compared to MBCP® (Supplementary Figure 1C). Our data are in agreement with results from other types of ceramic scaffolds, in which the presence of a high percentage of tricalcium phosphate compared to hydroxyapatite resulted in a faster release of calcium ions (Yuan et al., 2010).

In vitro co-culture systems

In vitro assays allow the study of complex biological processes by conducting experiments in a highly controlled system with the possibility to investigate cell-cell interactions and to isolate secreted growth factors and cytokines released by cells and that are technically hard to be identified *in vivo.* To assess if and how hBMSC seeded onto the two CaP scaffolds could differently regulate endothelial cell behaviour, we studied HUVEC proliferation, functionality and VEGF content in the described experimental settings*:*

hBMSCs – ceramics interaction affects endothelial cell proliferation by modulation of VEGF secretion

We evaluated HUVEC proliferation in the co-culture system described in Figure 1A. Significant increase in the number of HUVEC was observed in the cultures performed in the presence of BMSC seeded onto either MBCP® or MBCP^{+}® in comparison to HUVEC cultured

in the absence of scaffold or in the presence of scaffolds without cells (Figure 1B). Moreover, higher cell number was observed in the presence of BMSC seeded MBCP$^{+®}$ with the number of HUVEC in presence of the BMSC seeded into MBCP$^{®}$. No differences were observed when HUVEC cultured in SF medium or in the presence of no acellular scaffolds (Figure 1B). We observed an increased number of DAPI positive nuclei in the HUVEC culture in the presence of both BMSC seeded scaffolds. Figure 1C represents one group of pictures representative of three independent experiments. From the equivalent cultures, conditioned media were collected to verify the presence of specific cytokines and growth factors possibly involved in HUVEC proliferation/functionality. The enzymatic-linked immunosorbent assay (ELISA) for VEGF detection revealed the presence of this growth factor in the conditioned media obtained by BMSC seeded onto both ceramic CaP scaffolds. Higher level of secreted VEGF was observed in samples from BMSC seeded on MBCP$^{+®}$ in comparison to those to MBCP$^{®}$ (Figure 1D). Quantification of VEGF secreted by BMSC cultured in 2D were significantly lower than those obtained in 3D cultures of BMSC seeded onto ceramic scaffolds (data not shown).

HUVEC capillary formation as result of the cross-talk with BMSC seeded on ceramics

The ceramic scaffolds not seeded (controls) and seeded with BMSC were positioned at the bottom of multiwell plate and enclosed within matrigel. HUVEC were then placed on the matrigel upper surface. Illustration of the experiments is represented in figure 2A. Tube formation is typically quantified by measuring number, length and/or area of formed capillary-like structures observed in two-dimensional microscope. Compared to BMSC cultured onto MBCP$^{®}$, BMSC within MBCP$^{+®}$ conferred to HUVEC a higher sprouting and lumen formation capacity already after 6 hours (Figure 2B). After 24 hours, HUVEC in presence of BMSC seeded MBCP$^{+®}$ ceramics presented a significantly higher number of tubes formed in comparison to those cultured in presence of BMSC seeded MBCP$^{®}$. The differences in

promoting angiogenesis *in vitro* – i.e. formation of morphologically mature capillaries - can be observed in figure 2C. Neither acellular MBCP® nor MBCP+® were able to sustain capillary formation and long-term stability of the vascular networks.

Host vessel sprouting and homing into CaP scaffolds

Detection and quantification of blood vessels sprouted inside the explanted ceramic scaffolds were made using Mallory Trichrome staining (Figure 3). At early implantation time - figure 3A - (15 days; first row of inserts), a burst in the presence of blood vessel was observed in both scaffolds (stained in gold yellow), being MBCP+® penetrated by a higher number of bigger host sprouted vessels in comparison to MBCP®. Similar tendency was observed in 1 month explanted scaffolds (middle line inserts). MBCP+® show a considerably higher number of total blood vessels compared to MBCP® scaffold in the overall time. The scaffolds explanted after 2 months (last inserts) showed an analogous tendency although the total number of blood vessel per area has significantly decreased in both scaffolds. After the quantification of the total number of blood vessels inside both scaffolds (Figure 3B), we demonstrate that for all time points MBCP+® explants (grey columns) presented higher amount of blood vessels in comparison to MBCP® samples (black columns). MBCP® explants showed a continual reduction of blood vessels from 15 days until 2 months. The amount of blood vessels within MBCP+® scaffolds increased from 7 days to the 1 month (not in a statistically significant way). Afterwards, we observed a much lower number of blood vessels at 2 months.

Localization of human cells on ceramics explants: activation of calcium sensing receptor on hBMSC during bone deposition process

In situ hybridization was made to confirm the presence of the seeded BMSC in the constructs after 1 week implantation and to distinguish between host cells and cells derived from the

human seeded BMSC (Figure 4A). Tissue areas were divided in two distinct zones: (i) the internal area in direct contact with the scaffolds where cells undoubtedly show a strong positivity for human-specific Alu sequence; (ii) zones more external to the ceramics scaffolds, but adjacent to the bone deposited by the human cells, that are colonized by host murine cells (negative for the presence of human-specific Alu sequence).

Calcium released by ceramic scaffolds dissolution plays a crucial role in cell osteogenic commitment *in vivo* through Wnt/$Ca2^{+}$ signalling pathway (Chen et al., 2014). Therefore, we searched for the presence of active CaSr in the implanted BMSC seeded onto the two different CaP scaffolds (Figure 4B). After 1 week, a higher number of BMSC positive for active CaSr were observed in MBCP$^{+®}$ compared to MBCP$^{®}$ (Figure 4B). Positive cells were immediately adjacent to the ceramic scaffold.

In vivo neo-bone formation and maturation by BMSC seeded on the two ceramics

We tested hBMSC capacity to form bone within the two different ceramics in a well established ectopic bone formation model consisting in the subcutaneous implantation of cell-ceramic constructs in immuno-compromised mice (Muraglia et al., 1998a). BMSC seeded on both CaP ceramics gave rise to tissue-engineered ossicles with mineralized bone detectable after 1 and 2 months (Figure 5A). More specifically, in the MBCP$^{®}$ CaP scaffold, we observed a gradual bone deposition with the presence of few osteocytes established within ceramics in the 2 months explants. The newly formed bone was surrounded by connective tissue where few blood vessels were present. Host cells also colonized the control no cell-seeded scaffolds. However, at one month the explants showed the presence of a loose connective tissue in between granules. At 2 months the connective tissue was denser with parallel oriented fibres especially in areas adjacent to the scaffold, and no bone formation was observed (data not shown). Whereas well-organized structures commonly associated to mature bone, such as

osteons, were detectable in controls implanted scaffolds seeded with sheep BMSC (data not shown). Histomorphometric quantification of new-formed bone indicates an increase of bone formation with increased implantation time in both scaffolds, but also statistically significant differences between the two ceramics at both 1 and 2 month implantation (Figure 5B). Samples explants at 2 months were also prepared for histology according to a resin embedding technique, which allows the observation of bone deposition dynamics in non-decalcified samples (Canciani et al., 2015). It was possible to observe time dependent differences in the bone formation process within the two scaffolds (Figure 5 C). The 1 month MCBP® explants showed a rearrangement of the BMSC adjacent to the scaffold surface and the presence of an immature bone matrix (I.B.). At the same time, in the MCBP$^{+®}$ scaffolds a tracked line of mature bone (M.B.) with embedded osteocytes in contact with the scaffold surface was already clearly detectable. Above the mature bone, was present a thin row of unmineralized matrix – Osteoid (Os), product of osteoblast (Ob) activity localized on top of it. With increased implantation time, the mature bone areas became bigger and denser. In MBCP$^{+®}$, new-formed ossicles were surrounded by well-organized blood vessels (V).

In vivo BMP2 time dependent activation signalling

To investigate possible mechanisms of the enhanced *in vivo* osteogenesis in CaP scaffolds seeded with BMSC, we looked for the presence of BMP2 taking advantage of antibodies directed against the active human protein (Figure 6). Both after 1 and 2 months implantation, within MBCP$^{+®}$ scaffolds, but not within the MBCP®, the cells lining the ceramic scaffold showed an upregulation of BMP2 protein expression (Figure 6A and B, first line of inserts represents MBCP® and the second MBCP$^{+®}$ for the different explants). This prompted us to hypothesize that an initial CaSr activation in the MBCP$^{+®}$ scaffolds triggered a fast bone differentiation with activation of BMP2 pathway.

Discussion

Ectopic bone formation by implantation of hBMSCs seeded on different scaffolds is sustained by events such as osteoconduction and osteoinduction. Over time, the interaction between degradable ceramic scaffolds, hBMSCs and host heterogeneous milieu at the implant site has gained the attention of regenerative medicine and tissue engineering scientists. Initial angiogenesis is one of the key points to sustain the osteogenic differentiation of the implanted cells (S Ghanaati et al., 2011; Kanczler & Oreffo, 2008; Santos et al., 2008). In this study, we first addressed our attention to the capacity of hBSMCs on the ceramic scaffolds to sustain *in vitro* HUVEC neo-angiogenic properties. hBMSCs seeded into MBCP$^{+®}$ scaffold induced a significant increase in HUVEC mitogenesis compared to the MBCP$^{®}$ scaffolds ($p<0.001$). For both scaffolds, the absence of hBMSCs resulted in a significant ($p<0.001$) decrease in HUVEC number that can indicate that calcium by itself could not play a major role in endothelial cell growth. Given these findings, we cannot exclude the possibility that HUVEC calcium sensing receptors proteins (CaSr) might be activated by calcium ions released from ceramics but, even if this occurred, it was not sufficient to sustain *in vitro* HUVEC proliferation. In the co-culture system, quantified VEGF levels were statistically significantly higher in the presence of MBCP$^{+®}$ in comparison to MBCP$^{®}$. It is known that VEGF has a key role in preserving endothelial cell phenotype and viability that sustain vascular integrity (Liu et al., 2004; Masood et al., 2001; Mayer et al., 2005; Rosen, 2009; Simorre-Pinatel et al., 1994). hBMSCs seeded in CaPs primed the formation of lumen structures by HUVEC demonstrated by the quantification of capillary tubes. Capillary tube formation has been proved to be a well-recognized *in vitro* model to study neo-angiogenesis mechanisms (Grant et al., 1995; Herrmann et al., 2014; T Mirabella, Cilli, Carlone, Cancedda, & Gentili, 2011). These mechanisms are fundamental in bone formation process and a crucial requisite for bone sustainment (Kanczler & Oreffo, 2008; Kirkpatrick, Fuchs, & Unger, 2011). By this, several approaches have been proposed to raise

scaffold vascularization (Asahara et al., 1997; Jabbarzadeh et al., 2008; Kirkpatrick et al., 2011; Rouwkema, de Boer, & Van Blitterswijk, 2006; Verseijden et al., 2010). High level of vascularization during bone formation is crucial as the rate and extent of vascularization directly relates to bone growth. We showed that already after 15 days of implantation MBCP$^{+®}$ seeded with hBMSCs displayed higher presence of blood vessels compared to MBCP®. This was maintained over time with a final superior organization of vascular structures (Fig. 3A). Calcium ions can be involved in osteogenesis commitment and heterotopic bone formation. It has been shown that bioactive ceramics, at the site of implantation could create new apatite structures, which promotes cell spreading and osteogenic differentiation (Guy Daculsi, 2015). Moreover, the macropores convexity appears to act like a niche for the promotion of bone ingrowth and angiogenesis (Antoniac, 2014; Guy Daculsi & Layrolle, 2004). In CaPs the physical properties such as porosity and pore interconnectivity are crucial in vascularization, e.g., pore sizes directs new vessel formation and different pore sizes are reported to induce vessel formation with different diameters (Malhotra & Habibovic, 2016). In situ-hybridization demonstrated that cells attached to ceramic granules, mostly in the inner part of the scaffold and responsible for the initial neo-formation, are of human origin; while cells lining parallel to the granules in the external region are of mouse origin (Fig. 4A). The observation of human cells in close contact with ceramics strongly suggests a guidance of the ceramic nature and microenvironment on the behaviour of hBMSCs toward osteogenesis. Barradas et al. demonstrated that *in vitro* addition of calcium ions to hBMSCs increased their expression of bone related genes, thus indicating that calcium can act as an osteoinductive factor. Our *in vivo* results mirror these *in vitro* evidences. Presence of human cells in CaP adjacent regions and activation of calcium receptor in those cells, early process during calcification of the neo-formed tissue, was observed mainly in the 1 week explants. hBMSCs in CaP ceramic with high

in vitro calcium release presented higher levels of activation of calcium sensing receptor (Figure 4B).

The bone formation efficacy of hBMSCs on both ceramic scaffolds was evaluated and quantified up to 2 months (Figure 5A and B). In MBCP$^{+®}$ scaffolds at 1 month, hBMSCs generated bone tissue with parallel orientation to the ceramic surface with osteocytes (Oc) full embedded in their dense collagen matrix deposited by the aligned osteoblasts (Ob).

During development, vascularization precedes osteogenesis in both endochondral and intramembranous ossification processes (Kronenberg et al., 2003; Trueta et al.,1960; Zelzer et al., 2004). At late time, the presence of organized vascular structures with bone marrow inside the formed bone reinforces the significant role of calcium-released ions from the ceramic at both morphological-structure scale and molecular level. In agreement with previous data published by our laboratory (M Mastrogiacomo et al., 2007; Papadimitropoulos et al., 2007), both implanted acellular ceramics, *per se*, did not display any trace of deposited bone tissue during the observation period. These outcomes mirror some results obtained in osteoinductive studies in small animals where it was demonstrated that CaP ceramics induced bone formation only in two of eleven different inbred mouse strains (Ana M C Barradas, Yuan, et al., 2012).

Several authors demonstrated, with very elegant *in vitro* experiments a direct relationship between calcium cellular sensing level and BMP-2 expression during bone formation by hBMSCs. The *in vitro* acting mechanism is activated and up-regulated by an unknown calcium sensing protein similar to calcium sensing receptor (Aldebaran M Hofer, 2005; Kanaya, Nemoto, Sakisaka, & Shimauchi, 2013; Tada et al., 2010). Other indication of a faster and sustained osteogenic commitment conducted by CaP ceramics on cells was the observation of active hBMP2. This member of BMP family acts as an osteoinductive agent by activation of its receptor that thought SMAD-dependent and independent pathways leads to osteoblast differentiation of mesenchymal progenitor cells (Bais et al., 2009; Soltanoff, Yang, Chen, &

Li, 2009). Indeed, we observed a difference in the number of hBMP2 positive cells in the two explanted ceramics. Calcium released during CaP scaffold degradation can play a fundamental role in osteogenic commitment of seeded and nearby cells through Wnt/Ca2+ signalling pathway leading to BMP2 expression. It was reported that the activation of CaSr induces BMP2 synthesis and secretion via phosphatidylinoditol-3-kinase. Exclusion of CaSr totally inhibited BMP2 activation (Peiris, Pacheco, Spencer, & MacLeod, 2007). Moreover, we observed a higher number of positive human BMP2 cells on MBCP$^{+®}$ compared to those in MBCP$^{®}$, which re-enforces the idea that the *in vivo* up-regulation of BMP2 can be related with the up-regulation of CaSr.

Conclusions

We have shown that high content of β–TCP on ceramic scaffolds affects hBMSCs seeded cells ability both to sustain angiogenesis and to promote mature osteogenesis differentiation by an endochondral bone process.

Firstly, the release of calcium ions from CaP ceramics was related to a high secretion of VEGF in seeded hBMSCs, which acts in paracrine mode on endothelial cells priming mitogenesis and capillary tube formation. We showed that ectopically implanted scaffolds with a higher amount of β–TCP elicited superior and faster host vascular spreading and sustenance than the scaffold with a lower β–TCP content. The prompted hBMSCs osteogenesis could be triggered by calcium ions released from CaP scaffold in an ectopic mouse microenvironment. In this niche, Ca^{2+} ions drove a faster bone formation with an observed activation of hBMSCs calcium receptor. Bone formed by hBMSCs resulted to be more robust over time with upregulation of BMP2.

Our work highlights the importance of the ceramic scaffold composition in bone formation and maintenance by hBMSCs. These findings could guide future ceramics developments.

Acknowledgements

The authors gratefully acknowledge the financial support of the "GAMBA" EU-Project from FP7 framework (NMP3-Sl-2010-245993) and Italian Ministry of Education, University of Genoa.

References

Antoniac, I. V. (Ed.). (2014). *Handbook of Bioceramics and Biocomposites*. Cham: Springer International Publishing. https://doi.org/10.1007/978-3-319-09230-0

Asahara, T., Murohara, T., Sullivan, A., Silver, M., van der Zee, R., Li, T., … Isner, J. M. (1997). Isolation of putative progenitor endothelial cells for angiogenesis. *Science (New York, N.Y.)*, *275*(5302), 964–967. Retrieved from http://www.ncbi.nlm.nih.gov/pubmed/9020076

Bais, M. V, Wigner, N., Young, M., Toholka, R., Graves, D. T., Morgan, E. F., … Einhorn, T. A. (2009). BMP2 is essential for post natal osteogenesis but not for recruitment of osteogenic stem cells. *Bone*, *45*(2), 254–266. https://doi.org/10.1016/j.bone.2009.04.239

Barradas, A. M. C., Fernandes, H. A. M., Groen, N., Chai, Y. C., Schrooten, J., van de Peppel, J., … de Boer, J. (2012). A calcium-induced signaling cascade leading to osteogenic differentiation of human bone marrow-derived mesenchymal stromal cells. *Biomaterials*, *33*(11), 3205–3215. https://doi.org/10.1016/j.biomaterials.2012.01.020

Barradas, A. M. C., Monticone, V., Hulsman, M., Danoux, C., Fernandes, H., Tahmasebi Birgani, Z., … de Boer, J. (2013). Molecular mechanisms of biomaterial-driven osteogenic differentiation in human mesenchymal stromal cells. *Integrative Biology : Quantitative Biosciences from Nano to Macro*, *5*(7), 920–931. https://doi.org/10.1039/c3ib40027a

Barradas, A. M. C., Yuan, H. P., van Blitterswijk, C. A., & Habibovic, P. (2011). Osteoinductive Biomaterials: Current Knowledge of Properties, Experimental Models and Biological Mechanisms. *European Cells & Materials*, *21*, 407–429.

Barradas, A. M. C., Yuan, H. P., van der Stok, J., Le Quang, B., Fernandes, H., Chaterjea, A., … de Boer, J. (2012). The influence of genetic factors on the osteoinductive potential of calcium phosphate ceramics in mice. *Biomaterials*, *33*(23), 5696–5705. https://doi.org/Doi 10.1016/J.Biomaterials.2012.04.021

Barradas, A. M. C., Yuan, H. P., van der Stok, J., Quang, B. L., Fernandes, H., Chaterje, A., … de Boer, J. (2012). The influence of genetic factors on the osteoinductive potential of calcium phosphate ceramics in mice. *Biomaterials*, *33*(23), 5696–5705. https://doi.org/Doi 10.1016/J.Biomaterials.2012.04.021

Bianco, P., Cancedda, F. D., Riminucci, M., & Cancedda, R. (1998). Bone formation via cartilage models: the "borderline" chondrocyte. *Matrix Biology : Journal of the International Society for Matrix Biology*, *17*(3), 185–192. Retrieved from http://www.ncbi.nlm.nih.gov/pubmed/9707341

Cancedda, R., Bianchi, G., Derubeis, A., & Quarto, R. (2003). Cell therapy for bone disease:

A review of current status. *Stem Cells*, *21*(5), 610–619. https://doi.org/Doi 10.1634/Stemcells.21-5-610

Canciani, B., Ruggiu, A., Giuliani, A., Panetta, D., Marozzi, K., Tripodi, M., … Tavella, S. (2015). Effects of long time exposure to simulated micro- and hypergravity on skeletal architecture. *Journal of the Mechanical Behavior of Biomedical Materials*, *51*, 1–12. https://doi.org/10.1016/j.jmbbm.2015.06.014

Chen, Z. T., Wu, C. T., Gu, W. Y., Klein, T., Crawford, R., & Xiao, Y. (2014). Osteogenic differentiation of bone marrow MSCs by beta-tricalcium phosphate stimulating macrophages via BMP2 signalling pathway. *Biomaterials*, *35*(5), 1507–1518. https://doi.org/Doi 10.1016/J.Biomaterials.2013.11.014

Daculsi, G. (2015). Smart scaffolds: the future of bioceramic. *Journal of Materials Science. Materials in Medicine*, *26*(4), 154. https://doi.org/10.1007/s10856-015-5482-7

Daculsi, G., Fellah, B. H., Miramond, T., & Durand, M. (2013). Osteoconduction, Osteogenicity, Osteoinduction, what are the fundamental properties for a smart bone substitutes. *IRBM*, *34*(4–5), 346–348. https://doi.org/10.1016/j.irbm.2013.07.001

Daculsi, G., Laboux, O., Malard, O., & Weiss, P. (2003). Current state of the art of biphasic calcium phosphate bioceramics. *Journal of Materials Science-Materials in Medicine*, *14*(3), 195–200. https://doi.org/Doi 10.1023/A:1022842404495

Daculsi, G., & Layrolle, P. (2004). Osteoinductive Properties of Micro Macroporous Biphasic Calcium Phosphate Bioceramics. *Key Engineering Materials*, *254–256*, 1005–1008. https://doi.org/10.4028/www.scientific.net/KEM.254-256.1005

Daculsi, G., Miramond, T., Borget, P., & Baroth, S. (2012). Smart Calcium Phosphate Bioceramic Scaffold for Bone Tissue Engineering. *Key Engineering Materials*, *529–530*, 19–23. https://doi.org/10.4028/www.scientific.net/KEM.529-530.19

El Backly, R. M., Zaky, S. H., Muraglia, A., Tonachini, L., Brun, F., Canciani, B., … Mastrogiacomo, M. (2013). A platelet-rich plasma-based membrane as a periosteal substitute with enhanced osteogenic and angiogenic properties: a new concept for bone repair. *Tissue Engineering. Part A*, *19*(1–2), 152–165. https://doi.org/10.1089/ten.TEA.2012.0357

Espitalier, F., Vinatier, C., Lerouxel, E., Guicheux, J., Pilet, P., Moreau, F., … Malard, O. (2009). A comparison between bone reconstruction following the use of mesenchymal stem cells and total bone marrow in association with calcium phosphate scaffold in irradiated bone. *Biomaterials*, *30*(5), 763–769. https://doi.org/Doi 10.1016/J.Biomaterials.2008.10.051

Ferrara, N., Gerber, H. P., & LeCouter, J. (2003). The biology of VEGF and its receptors. *Nature Medicine*, *9*(6), 669–676. https://doi.org/Doi 10.1038/Nm0603-669

Ghanaati, S., Barbeck, M., Orth, C., Willershausen, I., Thimm, B. W., Hoffmann, C., … Kirkpatrick, C. J. (2010). Influence of β-tricalcium phosphate granule size and morphology on tissue reaction in vivo. *Acta Biomaterialia*, *6*(12), 4476–4487. https://doi.org/10.1016/j.actbio.2010.07.006

Ghanaati, S., Unger, R. E., Webber, M. J., Barbeck, M., Orth, C., Kirkpatrick, J. A., … Kirkpatrick, C. J. (2011). Scaffold vascularization in vivo driven by primary human osteoblasts in concert with host inflammatory cells. *Biomaterials*, *32*(32), 8150–8160. https://doi.org/Doi 10.1016/J.Biomaterials.2011.07.041

Goshima, J., Goldberg, V. M., & Caplan, A. I. (1991). The osteogenic potential of culture-

expanded rat marrow mesenchymal cells assayed in vivo in calcium phosphate ceramic blocks. *Clinical Orthopaedics and Related Research*, (262), 298–311. Retrieved from http://www.ncbi.nlm.nih.gov/pubmed/1984928

Grant, D. S., Kinsella, J. L., Kibbey, M. C., LaFlamme, S., Burbelo, P. D., Goldstein, A. L., & Kleinman, H. K. (1995). Matrigel induces thymosin beta 4 gene in differentiating endothelial cells. *Journal of Cell Science*, *108 (Pt 1*, 3685–3694. Retrieved from http://www.ncbi.nlm.nih.gov/pubmed/8719875

Herrmann, M., Binder, A., Menzel, U., Zeiter, S., Alini, M., & Verrier, S. (2014). CD34/CD133 enriched bone marrow progenitor cells promote neovascularization of tissue engineered constructs in vivo. *Stem Cell Research*, *13*(3 Pt A), 465–477. https://doi.org/10.1016/j.scr.2014.10.005

Hofer, A. M. (2005). Another dimension to calcium signaling: a look at extracellular calcium. *Journal of Cell Science*, *118*(Pt 5), 855–862. https://doi.org/10.1242/jcs.01705

Hofer, A. M., & Lefkimmiatis, K. (2007). Extracellular calcium and cAMP: Second messengers as "third messengers"? *Physiology*, *22*(5), 320–327. https://doi.org/Doi 10.1152/Physiol.00019.2007

Jabbarzadeh, E., Starnes, T., Khan, Y. M., Jiang, T., Wirtel, A. J., Deng, M., … Laurencin, C. T. (2008). Induction of angiogenesis in tissue-engineered scaffolds designed for bone repair: a combined gene therapy-cell transplantation approach. *Proceedings of the National Academy of Sciences of the United States of America*, *105*(32), 11099–11104. https://doi.org/10.1073/pnas.0800069105

Kanaya, S., Nemoto, E., Sakisaka, Y., & Shimauchi, H. (2013). Calcium-mediated increased expression of fibroblast growth factor-2 acts through NF-κB and PGE2/EP4 receptor signaling pathways in cementoblasts. *Bone*, *56*(2), 398–405. https://doi.org/10.1016/j.bone.2013.06.031

Kanczler, J. M., & Oreffo, R. O. C. (2008). Osteogenesis and angiogenesis: The potential for engineering bone. *European Cells & Materials*, *15*, 100–114. Retrieved from http://www.ncbi.nlm.nih.gov/pubmed/18454418

Khlusov, I. A., Karlov, A. V, Sharkeev, Y. P., Pichugin, V. F., Kolobov, Y. P., Shashkina, G. A., … Sukhikh, G. T. (2005). Osteogenic potential of mesenchymal stem cells from bone marrow in situ: role of physicochemical properties of artificial surfaces. *Bulletin of Experimental Biology and Medicine*, *140*(1), 144–152. Retrieved from http://www.ncbi.nlm.nih.gov/pubmed/16254641

Kirkpatrick, C. J., Fuchs, S., & Unger, R. E. (2011). Co-culture systems for vascularization--learning from nature. *Advanced Drug Delivery Reviews*, *63*(4–5), 291–299.

Komlev, V. S., Mastrogiacomo, M., Pereira, R. C., Peyrin, F., Rustichelli, F., & Cancedda, R. (2010). Biodegradation of Porous Calcium Phosphate Scaffolds in an Ectopic Bone Formation Model Studied by X-Ray Computed Microtomography. *European Cells & Materials*, *19*, 136–146. Retrieved from http://www.ncbi.nlm.nih.gov/pubmed/20349404

Kronenberg, H. M. (2003). Developmental regulation of the growth plate. *Nature*, *423*(6937), 332–336. https://doi.org/10.1038/nature01657

Le Nihouannen, D., Daculsi, G., Saffarzadeh, A., Gauthier, O., Delplace, S., Pilet, P., & Layrolle, P. (2005). Ectopic bone formation by microporous calcium phosphate ceramic particles in sheep muscles. *Bone*, *36*(6), 1086–1093. https://doi.org/10.1016/j.bone.2005.02.017

LeGeros, R. Z. (2008). Calcium Phosphate-Based Osteoinductive Materials. *Chemical Reviews*, *108*(11), 4742–4753. https://doi.org/Doi 10.1021/Cr800427g

Liu, Y., De Groot, K., & Hunziker, E. B. (2004). Osteoinductive implants: The Mise-en-scene for drug-bearing biomimetic coatings. *Annals of Biomedical Engineering*, *32*(3), 398–406. https://doi.org/Doi 10.1023/B:Abme.0000017536.10767.0f

Malhotra, A., & Habibovic, P. (2016). Calcium Phosphates and Angiogenesis: Implications and Advances for Bone Regeneration. *Trends in Biotechnology*, *34*(12), 983–992. https://doi.org/10.1016/j.tibtech.2016.07.005

Masood, R., Cai, J., Zheng, T., Smith, D. L., Hinton, D. R., & Gill, P. S. (2001). Vascular endothelial growth factor (VEGF) is an autocrine growth factor for VEGF receptor-positive human tumors. *Blood*, *98*(6), 1904–1913. Retrieved from http://www.ncbi.nlm.nih.gov/pubmed/11535528

Mastrogiacomo, M., Papadimitropoulos, A., Cedola, A., Peyrin, F., Giannoni, P., Pearce, S. G., … Cancedda, R. (2007). Engineering of bone using bone marrow stromal cells and a silicon-stabilized tricalcium phosphate bioceramic: evidence for a coupling between bone formation and scaffold resorption. *Biomaterials*, *28*(7), 1376–1384. https://doi.org/10.1016/j.biomaterials.2006.10.001

Mastrogiacomo, M., Scaglione, S., Martinetti, R., Dolcini, L., Beltrame, F., Cancedda, R., & Quarto, R. (2006). Role of scaffold internal structure on in vivo bone formation in macroporous calcium phosphate bioceramics. *Biomaterials*, *27*(17), 3230–3237. https://doi.org/10.1016/j.biomaterials.2006.01.031

Matsubara, T., Kida, K., Yamaguchi, A., Hata, K., Ichida, F., Meguro, H., … Yoneda, T. (2008). BMP2 Regulates Osterix through Msx2 and Runx2 during Osteoblast Differentiation. *Journal of Biological Chemistry*, *283*(43), 29119–29125. https://doi.org/Doi 10.1074/Jbc.M801774200

Mayer, H., Bertram, H., Lindenmaier, W., Korff, T., Weber, H., & Weich, H. (2005). Vascular endothelial growth factor (VEGF-A) expression in human mesenchymal stem cells: autocrine and paracrine role on osteoblastic and endothelial differentiation. *Journal of Cellular Biochemistry*, *95*(4), 827–839. https://doi.org/10.1002/jcb.20462

Mirabella, T., Cilli, M., Carlone, S., Cancedda, R., & Gentili, C. (2011). Amniotic liquid derived stem cells as reservoir of secreted angiogenic factors capable of stimulating neo-arteriogenesis in an ischemic model. *Biomaterials*, *32*(15), 3689–3699. https://doi.org/10.1016/j.biomaterials.2011.01.071

Mirabella, T., Poggi, A., Scaranari, M., Mogni, M., Lituania, M., Baldo, C., … Gentili, C. (2011). Recruitment of host's progenitor cells to sites of human amniotic fluid stem cells implantation. *Biomaterials*, *32*(18), 4218–4227. https://doi.org/10.1016/j.biomaterials.2010.12.028

Muraglia, A., Martin, I., Cancedda, R., & Quarto, R. (1998a). A nude mouse model for human bone formation in unloaded conditions. *Bone*, *22*(5 Suppl), 131S–134S. Retrieved from http://www.ncbi.nlm.nih.gov/pubmed/9600769

Muraglia, A., Martin, I., Cancedda, R., & Quarto, R. (1998b). A Nude Mouse Model for Human Bone Formation in Unloaded Conditions. *Bone*, *22*(5), 131S–134S. https://doi.org/10.1016/S8756-3282(98)00009-X

Novosel, E. C., Kleinhans, C., & Kluger, P. J. (2011). Vascularization is the key challenge in tissue engineering. *Advanced Drug Delivery Reviews*, *63*(4–5), 300–311. https://doi.org/Doi 10.1016/J.Addr.2011.03.004

Oreffo, R. O. C., & Triffitt, J. T. (1999). Future potentials for using osteogenic stem cells and biomaterials in orthopedics. *Bone*, *25*(2), 5s–9s. https://doi.org/Doi 10.1016/S8756-3282(99)00124-6

Papadimitropoulos, A., Mastrogiacomo, M., Peyrin, F., Molinari, E., Komlev, V. S., Rustichelli, F., & Cancedda, R. (2007). Kinetics of in vivo bone deposition by bone marrow stromal cells within a resorbable porous calcium phosphate scaffold: an X-ray computed microtomography study. *Biotechnology and Bioengineering*, *98*(1), 271–281. https://doi.org/10.1002/bit.21418

Peiris, D., Pacheco, I., Spencer, C., & MacLeod, R. J. (2007). The extracellular calcium-sensing receptor reciprocally regulates the secretion of BMP-2 and the BMP antagonist Noggin in colonic myofibroblasts. *American Journal of Physiology. Gastrointestinal and Liver Physiology*, *292*(3), G753-66. https://doi.org/10.1152/ajpgi.00225.2006

Place, E. S., Evans, N. D., & Stevens, M. M. (2009). Complexity in biomaterials for tissue engineering. *Nature Materials*, *8*(6), 457–470. https://doi.org/Doi 10.1038/Nmat2441

Quarto, R., Mastrogiacomo, M., Cancedda, R., Kutepov, S. M., Mukhachev, V., Lavroukov, A., … Marcacci, M. (2001). Repair of large bone defects with the use of autologous bone marrow stromal cells. *New England Journal of Medicine*, *344*(5), 385–386. https://doi.org/Doi 10.1056/Nejm200102013440516

Rosen, V. (2009). BMP2 signaling in bone development and repair. *Cytokine & Growth Factor Reviews*, *20*(5–6), 475–480. https://doi.org/Doi 10.1016/J.Cytogfr.2009.10.018

Rouwkema, J., de Boer, J., & Van Blitterswijk, C. A. (2006). Endothelial cells assemble into a 3-dimensional prevascular network in a bone tissue engineering construct. *Tissue Engineering*, *12*(9), 2685–2693. https://doi.org/10.1089/ten.2006.12.2685

Rubio, R., Abarrategi, A., Garcia-Castro, J., Martinez-Cruzado, L., Suarez, C., Tornin, J., … Rodriguez, R. (2014). Bone environment is essential for osteosarcoma development from transformed mesenchymal stem cells. *Stem Cells (Dayton, Ohio)*, *32*(5), 1136–1148. https://doi.org/10.1002/stem.1647

Santos, M. I., Tuzlakoglu, K., Fuchs, S., Gomes, M. E., Peters, K., Unger, R. E., … Kirkpatrick, C. J. (2008). Endothelial cell colonization and angiogenic potential of combined nano- and micro-fibrous scaffolds for bone tissue engineering. *Biomaterials*, *29*(32), 4306–4313. https://doi.org/Doi 10.1016/J.Biomaterials.2008.07.033

Simorre-Pinatel, V., Guerrin, M., Chollet, P., Penary, M., Clamens, S., Malecaze, F., & Plouet, J. (1994). Vasculotropin-VEGF stimulates retinal capillary endothelial cells through an autocrine pathway. *Investigative Ophthalmology & Visual Science*, *35*(9), 3393–3400. Retrieved from http://www.ncbi.nlm.nih.gov/pubmed/8056513

Soltanoff, C. S., Yang, S., Chen, W., & Li, Y.-P. (2009). Signaling networks that control the lineage commitment and differentiation of bone cells. *Critical Reviews in Eukaryotic Gene Expression*, *19*(1), 1–46. Retrieved from http://www.pubmedcentral.nih.gov/articlerender.fcgi?artid=3392028&tool=pmcentrez&rendertype=abstract

Tada, H., Nemoto, E., Kanaya, S., Hamaji, N., Sato, H., & Shimauchi, H. (2010). Elevated extracellular calcium increases expression of bone morphogenetic protein-2 gene via a calcium channel and ERK pathway in human dental pulp cells. *Biochemical and Biophysical Research Communications*, *394*(4), 1093–1097. https://doi.org/10.1016/j.bbrc.2010.03.135

Tampieri, A., Sprio, S., Sandri, M., & Valentini, F. (2011). Mimicking natural bio-

mineralization processes: A new tool for osteochondral scaffold development. *Trends in Biotechnology*, *29*(10), 526–535. https://doi.org/Doi 10.1016/J.Tibtech.2011.04.011

TRUETA, J., & LITTLE, K. (1960). The vascular contribution to osteogenesis. II. Studies with the electron microscope. *The Journal of Bone and Joint Surgery. British Volume*, *42–B*, 367–376. Retrieved from http://www.ncbi.nlm.nih.gov/pubmed/13855126

Tsai, T.-L., Wang, B., Squire, M. W., Guo, L.-W., & Li, W.-J. Endothelial cells direct human mesenchymal stem cells for osteo- and chondro-lineage differentiation through endothelin-1 and AKT signaling. *Stem Cell Research & Therapy*, *6*(1), 88. https://doi.org/10.1186/s13287-015-0065-6

Verseijden, F., Posthumus-van Sluijs, S. J., Pavljasevic, P., Hofer, S. O. P., van Osch, G. J. V. M., & Farrell, E. (2010). Adult human bone marrow- and adipose tissue-derived stromal cells support the formation of prevascular-like structures from endothelial cells in vitro. *Tissue Engineering. Part A*, *16*(1), 101–114. https://doi.org/10.1089/ten.TEA.2009.0106

Yao, H., Miura, Y., Yoshioka, S., Miura, M., Hayashi, Y., Tamura, A., … Maekawa, T. (2014). Parathyroid Hormone Enhances Hematopoietic Expansion Via Upregulation of Cadherin-11 in Bone Marrow Mesenchymal Stromal Cells. *Stem Cells*, *32*(8), 2245–2255. https://doi.org/Doi 10.1002/Stem.1701

Yuan, H., Fernandes, H., Habibovic, P., de Boer, J., Barradas, A. M. C., de Ruiter, A., … de Bruijn, J. D. (2010). Osteoinductive ceramics as a synthetic alternative to autologous bone grafting. *Proceedings of the National Academy of Sciences of the United States of America*, *107*(31), 13614–13619. https://doi.org/10.1073/pnas.1003600107

Zelzer, E., Mamluk, R., Ferrara, N., Johnson, R. S., Schipani, E., & Olsen, B. R. (2004). VEGFA is necessary for chondrocyte survival during bone development. *Development (Cambridge, England)*, *131*(9), 2161–2171. https://doi.org/10.1242/dev.01053

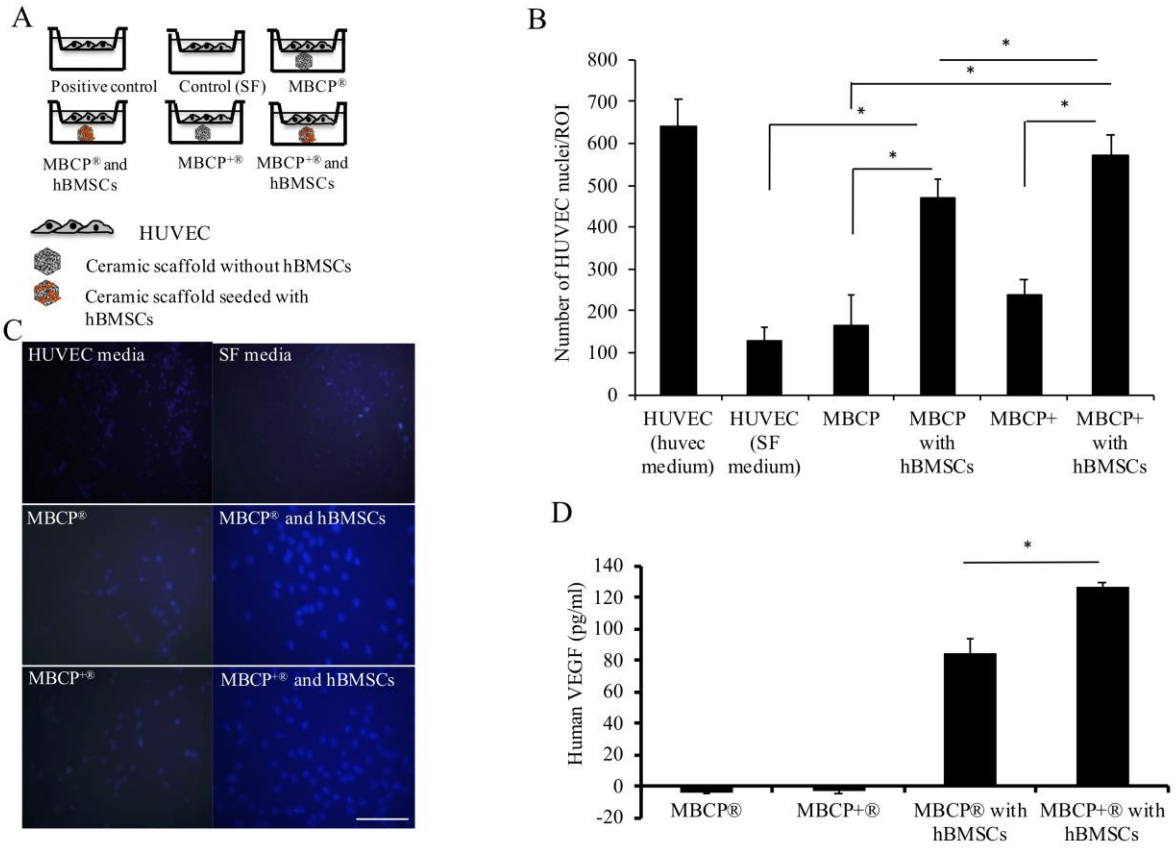

Figure 1 – A - Draft of experimental conditions for HUVEC proliferation assay using a non-direct co-culture system. - HUVECs cultured in HUVEC medium; - HUVECs cultured in Serum free medium (Sf); - HUVECs cultured in Sf medium exposed to MBCP® supernatant; - HUVECs cultured in Sf medium exposed to MBCP® seeded with hBMSCs supernatant; - HUVECs culture in SF medium exposed to MBCP$^{+®}$ supernatant; -HUVECs cultured in Sf medium exposed to MBCP$^{+®}$ seeded with hBMSCs supernatant. B - Quantification of HUVEC nuclei number for each culture conditions. Data acquired from four independent experiments. C - Representative images of HUVEC stained nuclei co-cultured under different conditions; - HUVEC cultured in standard HUVEC media, - HUVEC cultured in Sf media, - HUVEC cultured in presence of MBCP®, - HUVEC cultured with hBMSCs seeded into MBCP®, - HUVEC cultured in presence of MBCP$^{+®}$, - HUVEC cultured with hBMSCs seeded into MBCP$^{+®}$. D - Vascular endothelial growth factor (VEGF) quantification by ELISA, (n=3). *, figure 1B 1 way ANOVA (Nonparametric with post test TUKEY using family error rate of 0.05 value is statistically significant; * figure 1D t-test $p < 0.001$ is statistically significant. Scale bar = 100μm.

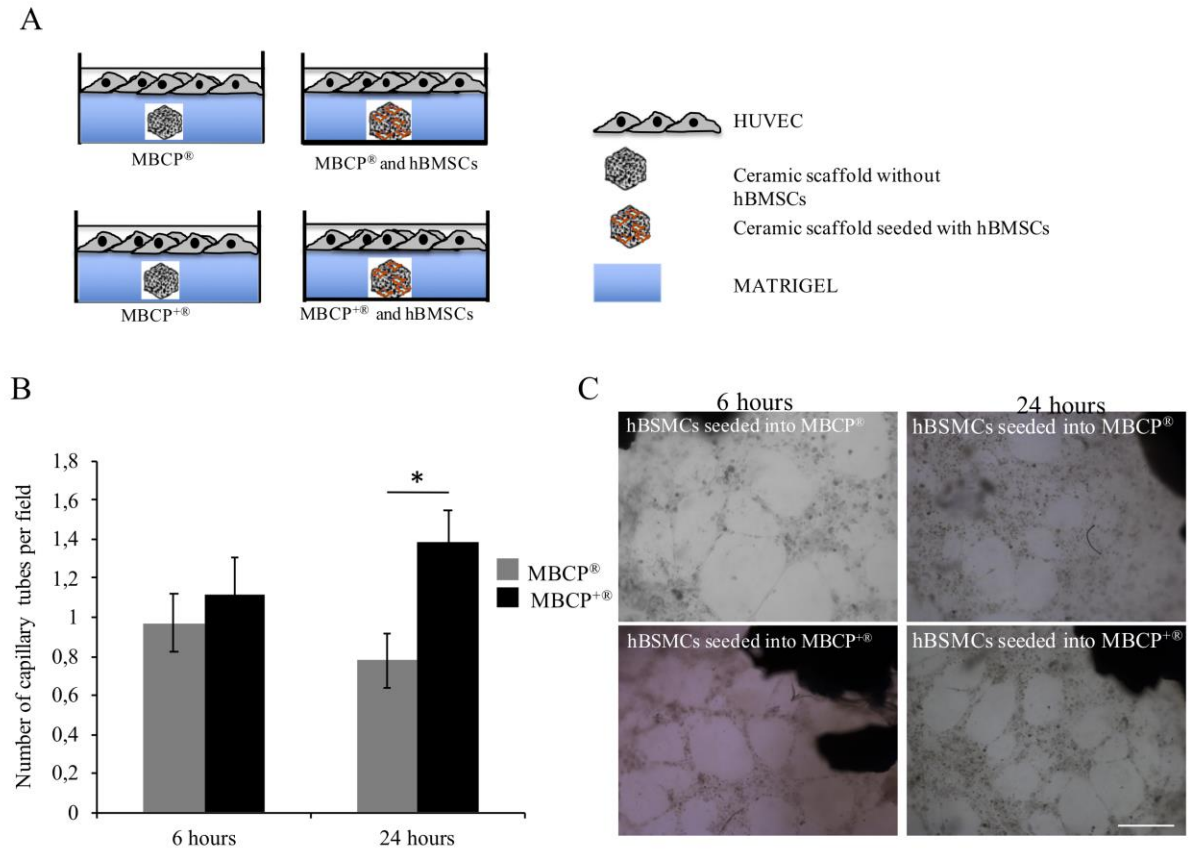

Figure 2 – HUVEC *in vitro* capillary tube formation. A - Draft of experimental conditions for HUVEC proliferation assay using a non-direct co-culture system in matrigel. - HUVECs cultured in Sf medium exposed to MBCP® supernatant; - HUVECs cultured in Sf medium exposed to MBCP® seeded with hBMSCs supernatant; - HUVECs culture in Sf medium exposed to MBCP$^{+®}$ supernatant; - HUVECs cultured in Sf medium exposed to MBCP$^{+®}$ seeded with hBMSCs supernatant. B - Over time quantification of HUVEC capillary tubes formed per region of interest (ROI) on the different conditions. C - Representative images of HUVEC seeded into the top layer of Matrigel co-cultured on the different conditions; Huvec in presence of hBSMCs seeded into MBCP® (first row); Huvec in presence of hBMSCs seeded into MBCP$^{+®}$ (second row). Microscope pictures were acquired after 6 and 24 hours of co-culture. Data from three independent experiments. *, t-test with $p < 0.001$ is statistically significant. Scale bar = 100µm.

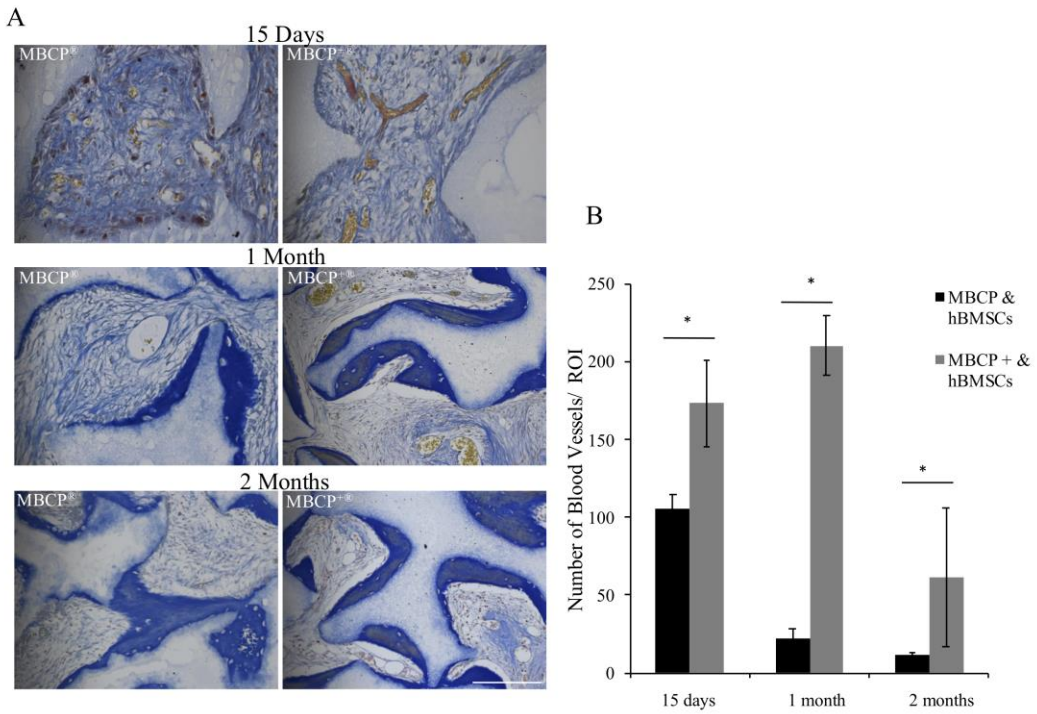

Figure 3 - Detection of vascular structures sprouted into the different ceramic scaffolds seeded with hBMSCs. A - Histological sections of explants stained with Mallory's trichome: MBCP® ceramics with hBMSCs after 2 weeks, 1 and 2 months respectively (left); and MBCP^{+}® ceramics with hBMSCs after 2 weeks, 1 and 2 months (right). B - Quantification of the number of blood vessels inside both different ceramic scaffolds over time. Error bars represent standard deviations. Asterisk (*) indicate statistical difference (t-test) $p < 0.05$. Scale bar = 100µm

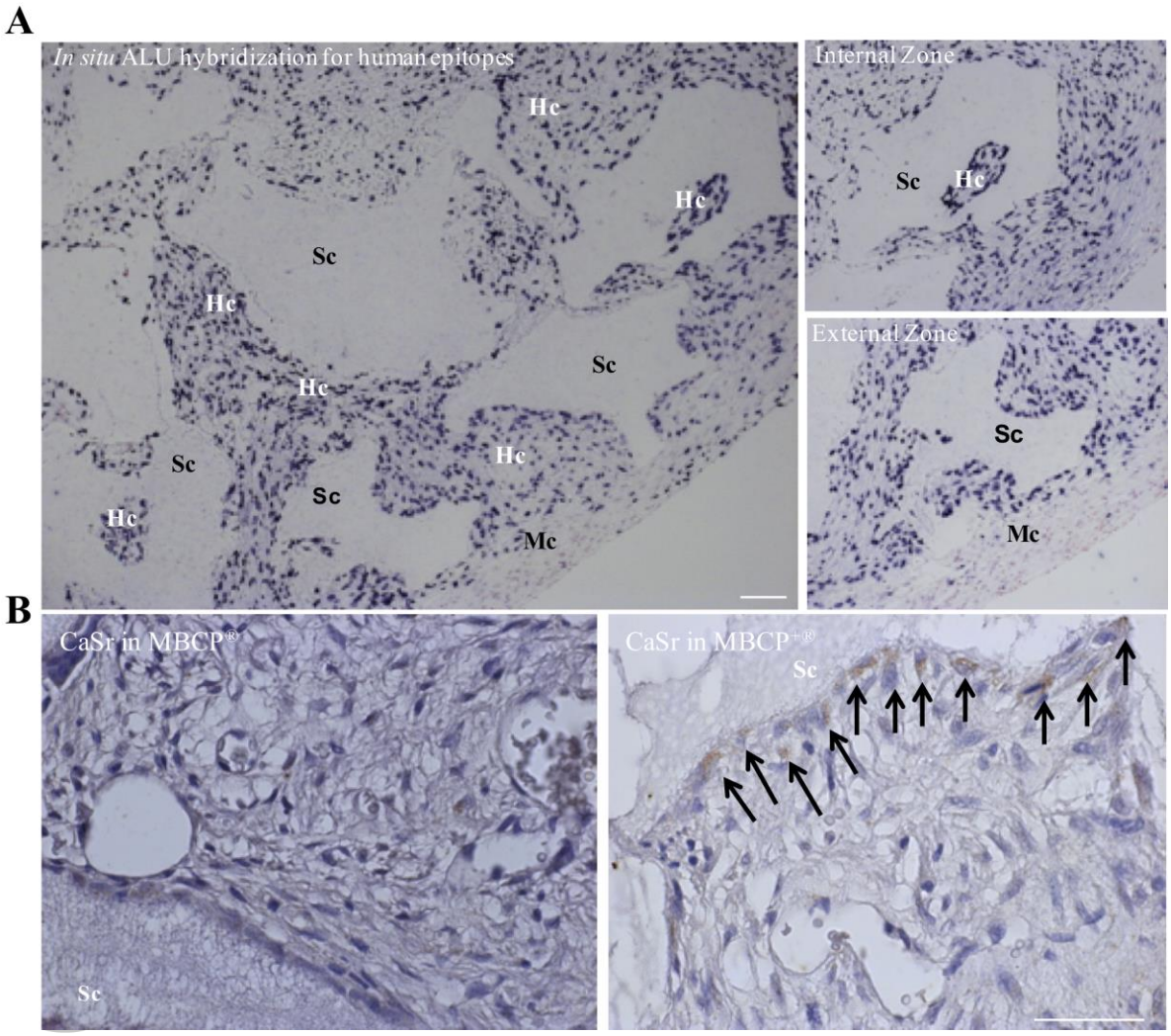

Figure 4 – Histological analysis of the in vivo engineered tissue in both calcium phosphate ceramics after 2 weeks. A - In situ Hybridization for human ALU repeated sequence; - large spectrum of all cellular populations within the ceramic; detailed visualization of human (internal zone) and mice (external zone) cells present into the calcium phosphate scaffolds. Scale bar = 100µm. B - Immune detection of CaSr active protein on implanted hBMSCs; - MBCP® ceramic scaffold and - MBCP$^{+®}$ respectively. Black arrows indicate the positive human cells on MBCP$^{+®}$ for hCaSr immune peroxidase. H&E was used as counterstaining. Scale bar = 100µm. Sc – Scaffold; Hc – Human Cells; Mc – Mice cells. Scale bar = 100µm.

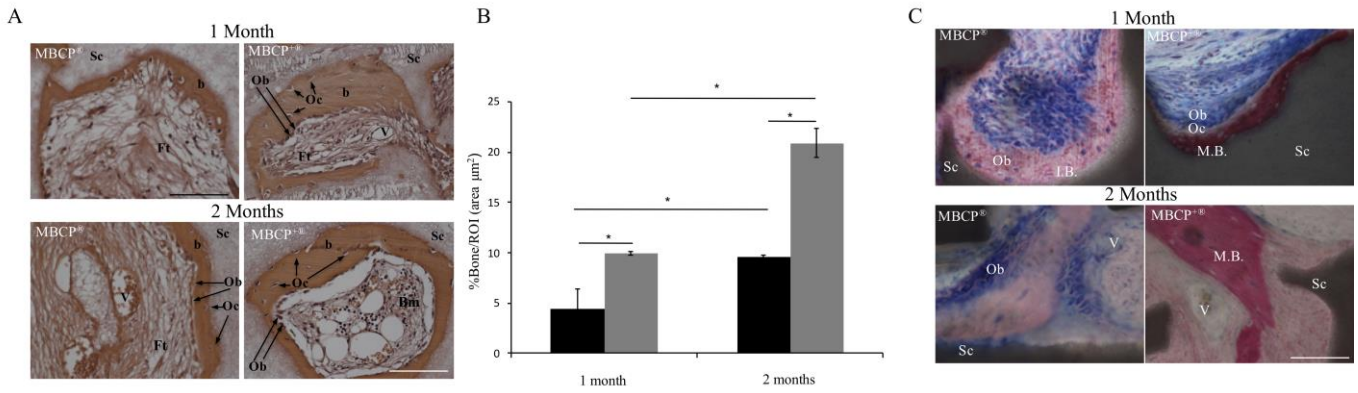

Figure 5 - Osteogenic differentiation of hBMSCs on calcium phosphate scaffolds. A - Histological sections stained Hematoxylin and Eosin (H&E) of explants; MBCP® with hBMSCs after 1 and 2 months respectively (left); MBCP^{+}® ceramics with hBMSCs after 1 and 2 months respectively (right). B - Quantification of bone area formed within different ceramics over time. C - Osteogenic differentiation potential of hBMSCs on both calcium phosphate ceramics on non-decalcified explants; Histological sections stained with Van Geison MBCP® and MBCP^{+}®, both loaded with bBMSCs implanted for 1 and 2 months respectively. Sc – scaffold; Ft – fibrotic tissue; Oc – osteocytes; Ob – osteoblasts; Os – osteoide; V – vessels; M.B. – Mature bone; I.B. – Immature bone and BM – bone marrow. The error bars represents standard deviations. Asterisk (*) denotes statistical difference in t-test with $p < 0.05$. Scale bar = 100µm

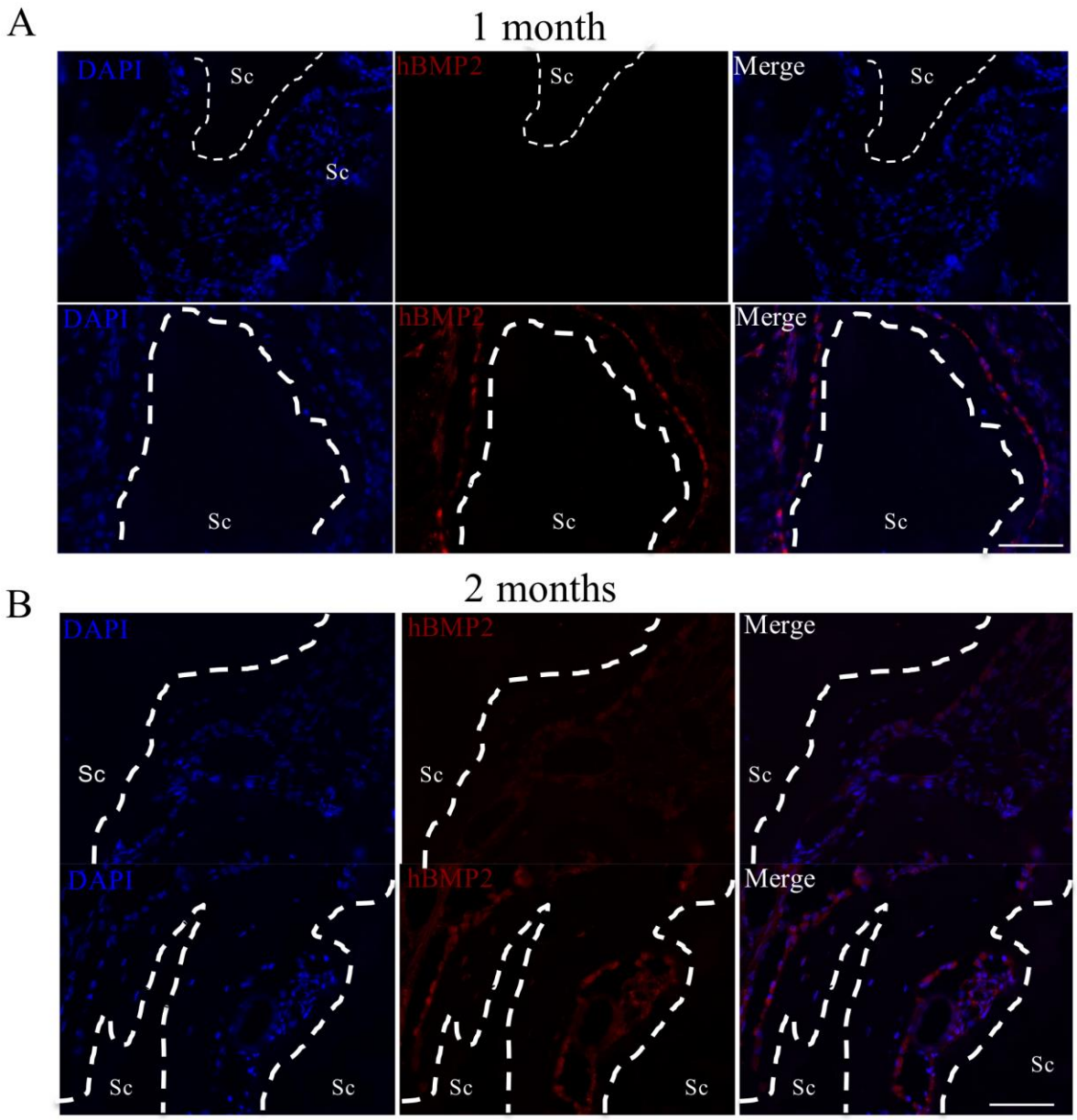

Figure 6 – Immunofluorescence detection of hBMP2 on calcium phosphate ceramics explants. Fluorescence microscopy images of hBMP2 on human BMSCs seeded into MBCP® (1-3 row) and MBCP^{+}® (2-4 row) CaP ceramics respectively at 1 month (A) and two months (B). DAPI (4',6-diamidino-2-phenylindole) was used as nuclear acid staining. Dashed lines label the scaffold (Sc). Scale bar = 100µm.